Multistability and hysteresis in the climate-cryosphere system under orbital forcing

Reinhard Calov and Andrey Ganopolski

Potsdam Institute for Climate Impact Research, Potsdam, Germany

[1] Using the Earth system model of intermediate complexity CLIMBER-2 we studied the stability diagram of the climate-cryosphere system in the phase space of Milankovitch forcing (maximum summer insolation at 65°N, abbreviated as MF). We have shown that the equilibrium response of the climate-cyrosphere system to MF reveals pronounced hysteresis behavior within the range of Earth's orbital parameters. Depending on MF, the climate-cryosphere system has either one (glacial or interglacial) or two different equilibrium states. The MF thresholds of the transitions between the two states depend on parameterizations of ice-sheet dynamics, but are rather insensitive to the choice of the orbital parameters used to obtain the same value of MF. A change of atmospheric CO_2 concentration from its interglacial to the glacial value, shifts the hysteresis curve by about 15 W/m^2. These results provide an important support to the conceptual models of glacial cycles based on multistability and hysteresis behavior.

1. Introduction

[2] In spite of considerable progress in studies of past climate changes, the nature of vigorous climate variations observed during the past several million years remains elusive. A variety of different astronomical theories, among which the Milankovitch theory [*Milankovitch*, 1941] is the best known, suggest changes in Earth's orbital parameters as a driver or, at least, a pacemaker of glacial-interglacial climate transitions. However, the mechanisms which translate seasonal and strongly latitude-dependent variations in the insolation into the global-scale climate shifts between glacial and interglacial climate states are the subject of debate. In a number of previous studies [e.g. *Imbrie and Imbrie*, 1980; *Oerlemans*, 1980; *Pollard*, 1982; *Saltzman*, 2002 and cited therein] it was shown that given a sufficient degree of non-linearity, conceptual and simplified models of the climate-cryosphere system under orbital forcing are able to reproduce some important features seen in paleoclimatic records, in particular the presence of a pronounced 100,000 yr cyclicity. Recently, *Paillard* [1998; 2001] proposed that observed glacial-interglacial climate variations can be explained by invoking such features of strongly nonlinear systems as multistability and hysteresis behavior. Paillard's model gives a rather good fit to the ice volume variations observed for the past million years. However, in these works Paillard did not specify which mechanisms and components of the Earth system are responsible for such strongly non-linear behavior.

[3] The possibility of a strong non-linearity of the Earth system and the existence of hysteresis behavior have already been proposed in early climate modeling studies. *Budyko* [1972] using an energy balance model showed that depending on insolation, the Earth system can attain either fully glaciated ("snow-ball Earth") or ice-free states, and that there is a range of insolation values where both equilibria exist. This hysteresis behavior was confirmed also with more sophisticated climate models [e.g. *Stone and Yao*, 2004]. Another well-known type of hysteresis is related to the response of the Atlantic thermohaline circulation to freshwater flux and was simulated with different models [e.g. *Stocker and Wright*, 1991; *Rahmstorf*, 1995; *Ganopolski and Rahmstorf*, 2001]. Recently, *Pollard and DeConto* [2005] demonstrated hysteresis of the Antarctic ice sheet in the phase space of atmospheric CO_2 concentration. The existence of hysteresis in the phase

space of Milankovitch forcing was postulated in the conceptual model of *Paillard* [1998] but has not been corroborated so far with geographically explicit climate-cryosphere models. In *Calov et al.* [2005], we demonstrated that glacial inception represents a bifurcation transition in the climate-cryosphere system and found multiple equilibria under present-day orbital configuration and pre-industrial atmospheric CO_2 concentration. Here, we present a systematic analysis of the stability diagram of the climate-cryosphere system in the MF space. Our study provides strong support to the idea of a strongly non-linear response of the climate-cryosphere system to the MF and the presence of thresholds and multiple equilibria.

2. Model and Method

[4] For the simulations, we used the Earth system model of intermediate complexity CLIMBER-2 [*Petoukhov et al*, 2000], which includes atmosphere, ocean, land surface, terrestrial vegetation, and inland-ice components. The latter is represented by the 3-D polythermal ice-sheet model SICOPOLIS [*Greve*, 1997]. A coarse resolution climate component and a high-resolution ice-sheet component are coupled bi-directionally via a physically based surface energy and mass balance interface [*Calov et al.*, 2005]. The ice-sheet model is only applied to the Northern Hemisphere, and no changes in the Antarctic ice sheet were assumed in this study. In *Calov et al.* [2002] we have shown that for realistic simulation of Heinrich events it is necessary to allow large sliding velocities over land areas covered by deformable sediments. In this study we use this version of the ice-sheet model as the basic one.

[5] Using the CLIMBER-2 model, we traced the existence of different equilibrium states under different orbital configurations and CO_2 concentrations. We chose the maximum summer insolation at 65°N, referred to as Milankovitch Forcing (MF) in this paper, as a representative proxy for the orbital forcing. Since the same value of MF can be obtained with different combinations of orbital parameters (precession, obliquity and eccentricity), one has to decide on a method to vary MF. In most of our experiments, we chose the following procedure: we fixed obliquity at its averaged value of 23°, considered only the "warm" and "cold" Earth orbits (Earth in perihelion or aphelion at the time of boreal summer solstice), and changed eccentricity within its natural range of variations

(from 0 to 0.06). When increasing eccentricity from zero to the maximum value for the "warm" orbit, we obtain MF in the range from 488 to 552 W/m^2, while when doing the same for the "cold" orbit we obtain MF in the range from 488 to 434 W/m^2, thereby this technique allows us to span the complete range of MF variations occurring during past several million years.

[6] We used two different techniques for the numerical analysis of the stability diagrams. One technique is based on multiple equilibrium runs for a set of different values of external forcing and initial conditions. Another technique is based on slow changes of external forcing in both directions [*Rahmstorf*, 1995]. The second technique is computationally less expensive than the first one, and allows the tracing of different branches of equilibrium solution and identification of bifurcation points. However, it is *a priori* unknown which rate of change of external forcing is slow enough to trace the stability diagram accurately enough. Although the typical time scale of the climate system can be estimated on the basis of general considerations, in the vicinity of transition points, as will be shown below, the time scale of the system response to external forcing increases drastically. Moreover, the standard hysteresis analysis does not guarantee to locate all possible equilibrium states, and it is possible that some equilibria are not accessible from the two main branches of the hysteresis curve [e.g. *Bauer et al.*, 2004]. Hence, we here employed both techniques to check the consistency between results obtained with both methods.

3. Results

[7] Applying the first technique, we performed a number of equilibrium experiments for the "cold" and "warm" orbital configurations and for the range of eccentricity from 0 to 0.06 with an increment of 0.01. Near the bifurcations we refined the increment to 0.002. Each run lasted 200,000 model years. The atmospheric CO_2 concentration was kept constant at its typical interglacial value of 280 ppm. In the first set of the equilibrium experiments, we used modern climate with an ice-free Northern Hemisphere as the initial conditions. For a broad range of MF, this solution is stable, i.e. the equilibrium climate states for different MF have very similar climate and small ice volume associated with the Greenland ice sheet only (Fig. 1a). However, for MF values below the critical

threshold S_I, the interglacial climate state becomes unstable and the ice sheets start to grow both over North America and Eurasia. The new equilibrium state attained by the climate system differs drastically from the modern one, with a total amount of ice sheets exceeding the reconstructed volume of the ice sheets in the Northern Hemisphere at the Last Glacial Maximum (ca. 21,000 years ago) by a factor two, and with a global temperature of 5°C lower than at present. To trace the second branch of equilibrium solutions, we used an equilibrium state obtained for the lowest value of MF (434 W/m^2) as the new initial condition, and repeated the experiments for the whole range of MF. The equilibrium solutions for both initial conditions precisely coincide for high (above 500 W/m^2) and low (below 460 W/m^2) values of MF, indicating that the climate-cryosphere system is in monostable regimes for high and low MF. However, for an intermediate range of MF (which encompasses both the averaged value of MF equal to 495 W/m^2, and the present-day MF value of 480 W/m^2), there are two distinct equilibrium states: one glacial and one interglacial equilibrium, see also Fig. 2a,b.

[8] We also performed a stability analysis using the second technique with a gradual change of MF. We started from the highest MF value and the interglacial climate state as initial conditions. We first reduced MF from its maximum to minimum value, and then increased it again with the rates of MF changes of 0.1 W/m^2 per 1000 years or 0.02 W/m^2 per 1000 years near the bifurcations. The tracing of a complete hysteresis loop required 3,840,000 model years in this experiment. As seen in Fig. 1, the individual equilibrium and continuous quasi-equilibrium solutions obtained using both techniques match well.

[9] To test our *a priori* assumption that the equilibrium states are primarily controlled by MF, irrespectively of the combination of orbital parameters used to obtain a given value of MF, we performed a number of additional equilibrium simulations where we used different combinations of orbital parameters. In particular, we performed two sets of experiments identical to those described above, except that we used two other obliquity parameters (22° and 24°) instead of 23°. We also traced the hysteresis in MF space by setting eccentricity to its maximum value of 0.06 and varying the precessional angle (the angle between vernal equinox and perihelion) from -90° to 90°. In this way we also cover the whole range of MF, but with a very different spatial and temporal distribution of insolation as compared to the first experiment. In all these experiments (not shown) we

obtained hysteresis curves very similar to Fig. 1, only somewhat shifted in MF space. These results indicate that MF is indeed a good proxy for the orbital forcing.

[10] To assess the role of the internal instability of ice sheets introduced by parameterization of fast sliding over sediment areas, we performed an additional set of experiments where this parameterization was switched off, whereby only slow sediment sliding applied. As seen in Fig. 1a,c, results of these experiments differ drastically from the standard model version. The equilibrium "glacial" solution is characterized by much thicker ice sheets, with the total volume of the Northern Hemisphere ice sheets about 50% higher than in the standard model version. Even more important, the hysteresis loop is much broader in the case of slow-sliding ice. This clearly illustrates that extremely thick ice sheets, simulated when internal ice-sheet instability is suppressed, are not susceptible to MF, and that the ice sheets can melt in the case of slow-sliding ice only under extremely high MF. This could explain problems with the simulation of glacial terminations in many climate-ice sheet models, and indicates the importance of the internal instability of ice sheets for the termination of glacial cycles.

[11] To assess the role of the glacial drop in the atmospheric CO_2 concentration, we performed an additional set of experiments identical to those runs explained at the beginning of this section, but with the glacial atmospheric CO_2 concentration of 200 ppm. In this case we used only the first technique, i.e. we performed a set of equilibrium simulations. It can be seen by direct comparison of Fig. 1b with Fig. 1a that the stability diagram looks qualitatively the same as in the case of interglacial atmospheric CO_2 concentration, but it is shifted towards high MF values by approximately 15 W/m^2. These experiments demonstrate that although the CO_2 concentration is an important factor in climate dynamics, the hysteresis loop remains within a range of realistic MF for any CO_2 concentration observed during the glacial cycles.

[12] The change of the response time of the climate-cryosphere system under different MF is illustrated in Fig. 3. The nearer MF approaches the bifurcation, the longer the climate-cryosphere system response time becomes. Far away from the bifurcation the response time has broadly the same value for varying MF and is of the order of tens of thousands of years (curve 1 in Fig. 3). The MF corresponding to curve 2 in Fig. 3 lies nearer the bifurcation than the MF of curve 1 and has thus with about 100,000 yrs a rather

long response time. The simulation which corresponds to curve 3 has an MF which is located the nearest to the bifurcation. Therefore, its response time with at least 200,000 years is the longest one.

4. Discussion and Conclusions

[13] Results of a set of numerical experiments with the CLIMBER-2 model demonstrate that as a first approximation the type and number of different equilibrium states depend only on the maximum summer insolation at 65°N. We found that the stability diagram is robust in the phase space of MF and not very sensitive to the way the orbital parameters are varied to obtain the range of MF used in the experiments. The stability diagram experiences systematic shifts to the right (left) with decreased (increased) CO_2 concentration, but the magnitude of this shift for the maximum range of glacial-interglacial atmospheric CO_2 concentration is only about 10% of the total range of MF (over million years time span). This clearly shows that MF exerts the primary control on the stability and possible equilibria of the climate-cryosphere system.

[14] It is important to realize that stability diagrams do not necessarily represent the true trajectory of the variables of a given dynamic system in its phase space, which in our case is the climate-cryosphere system in the MF phase space with time-varying orbital parameters. The primary reason for this is the long equilibration time of the climate-cryosphere system (Fig. 3), which has at least the same order of magnitude (or longer) as the dominant periodicities of the orbital forcing, i.e. 20,000 and 40,000 yrs. This is why the upper branch of stability probably cannot be reached during a glacial cycle. At the same time, the lower branch (interglacial state) is achieved after each or at least some terminations, and the system stays in the interglacial state for several thousand to several tens of thousands of years. The stability diagram clearly shows that as soon as the interglacial state is fully achieved, the system will stay in this state until MF falls below a critical threshold value S_I (Fig. 1). At the same time, it is important to realize that although S_I represent a bifurcation point of climate-cryosphere system, crossing S_I does not imply an instantaneous glaciation of the Earth. Our experiments show that in the close (left) proximity of S_I, the characteristic time scale of the system is very large (up to several hundred thousand years), and it theoretically approaches infinity when $S \rightarrow S_I$.

This is why, if the transient evolution of climate-cryosphere system under varying orbital parameters is considered, the crossing of threshold value S_I is only a necessary but is not a sufficient condition for the development of large-scale Northern Hemisphere glaciation. In the transient simulation of the last glacial inception by *Calov et al.* [2005], the inland ice in the Northern Hemisphere grows very slowly after crossing S_I, and only after MF drops several tens of W/m^2 below S_I does an abrupt increase of ice cover occur. Since for interglacial CO_2 concentration, the value of S_I is lower than the time-averaged value of MF, the MF can stay below S_I for no longer than half a precessional cycle. This is why the magnitude of ice growth during glacial inception depends strongly on the depth of the temporal MF minimum and the response of CO_2 to the initiation of ice sheets, which was also shown by *Loutre and Berger* [2000]. Interestingly enough, the value of S_I in our model is close to the present-day MF and to that which was used in Paillard's model.

[15] Among a number of feedbacks, the ice-surface elevation mass-balance feedback [*Weertman*, 1976] and the ice-albedo feedback [*North*, 1975] are both crucial important mechanism amplifying the transition from interglacial to glacial climate. This was also shown with simulations of last glacial inception by *Calov et al.* [2005]. In particular, they demonstrated that there is glacial inception, but with diminished ice cover, if the ice-sheet module in CLIMBER-2 is switch-off, i.e., the ice-albedo feedback is the only feedback in ice covered regions. In future work, one could try to quantify the contribution of these effects in a detailed analysis. An interesting peculiarity of analytical ice-sheet-stability studies is the existence of instable solutions [e.g. *North*, 1975; *Weertman*, 1976]. Such unstable branches cannot be found with our procedure as it is.

References

Bauer, E., A. Ganopolski, M. Montoya (2004), Simulation of the cold climate event 8200 years ago by meltwater outburst from Lake Agassiz, *Paleoceanography, 19*(3), PA3014, doi:10.1029/2004PA001030.

Budyko, M. I. (1972), The future climate. *Trans. Amer. Geophys. Union, 53*, 868-874.

Calov, R., A. Ganopolski, V. Petoukhov, M. Claussen, and R. Greve (2002), Large-scale instabilities of the Laurentide ice sheet simulated in a fully coupled climate-system model. *Geophys. Res. Lett., 29*(24), 2216, doi: 10.1029/2002GL016078.

Calov, R., A. Ganopolski, M. Claussen, V. Petoukhov, and R. Greve (2005), Transient simulation of the last glacial inception. Part I: glacial inception as a bifurcation of the climate system, *Clim. Dyn., 24*(6), 545-561, doi:10.1007/s00382-005-0007-6.

Ganopolski, A., and S. Rahmstorf (2001), Rapid changes of glacial climate simulated in a coupled climate model, *Nature, 409,* 153-158.

Greve, R. (1997), Application of a polythermal three-dimensional ice sheet model to the Greenland ice sheet: Response to steady-state and transient climate scenarios, *J. Clim., 10*, 901-918.

Imbrie, J. and J. Z. Imbrie (1980), Modeling the climatic response to orbital variations, *Science, 207*, 943-953.

Loutre, M. F., and A. Berger (2000), Future climatic changes: are we entering an exceptionally long interglacial?, *Clim. Change, 46*, 61-90.

Milankovitch (1941), *Kanon der Erdbestrahlung und seine Anwendung auf das Eiszeitenproblem,* Académie royale serbe, Édition speciale, Belgrade.

North, G. R. (1975), Analytical solution to a simple climate model with diffusive heat transport, *J. Atmos. Sci., 32*, 1301-1307.

Oerlemans, J. (1980), Model experiments on the 100,000-yr glacial cycle, *Nature, 287*, 430-432.

Paillard, D. (1998), The timing of Pleistocene glaciations from a simple multiple-state climate model, *Nature, 391*, 378-381.

Paillard, D. (2001), Glacial cycles: Toward a new paradigm, *Rev. Geophys., 39*, 325-346.

Petoukhov, V., *et al* (2000), CLIMBER-2: a climate system model of intermediate complexity. Part I: model description and performance for present climate, *Clim. Dyn., 16*, 1-17.

Pollard, D. (1982), A simple ice-sheet model yields realistic 100 kyr glacial cycles, *Nature, 296*, 334-338.

Pollard, D., and R. M. DeConto (2005), Hysteresis in Cenozoic Antarctic ice-sheet variations, Glob. Planet. Change, 45, 9-21.

Rahmstorf, S. (1995), Bifurcations of the Atlantic thermohaline circulation in response to changes in the hydrological cycle, *Nature, 378*, 145-149.

Saltzman, B. (2002), *Dynamical Paleoclimatology, Int. Geophys. Ser.,* vol. 80, 354p, Academic Press, San Diego.

Stocker, T. F., and D. G. Wright (1991), Rapid transitions of the ocean's deep circulation induced by changes in surface water fluxes, *Nature, 351*, 729-732.

Stone, P. H., and M. S. Yao (2004), The ice-covered Earth instability in a model of intermediate complexity, *Clim. Dyn., 22*(8), 815-822, doi:10.1007/s00382-004-0408-y.

Weertman J. (1976), Milankovitch solar radiation variations and ice age ice sheet sizes, *Nature, 261*, 17-20.
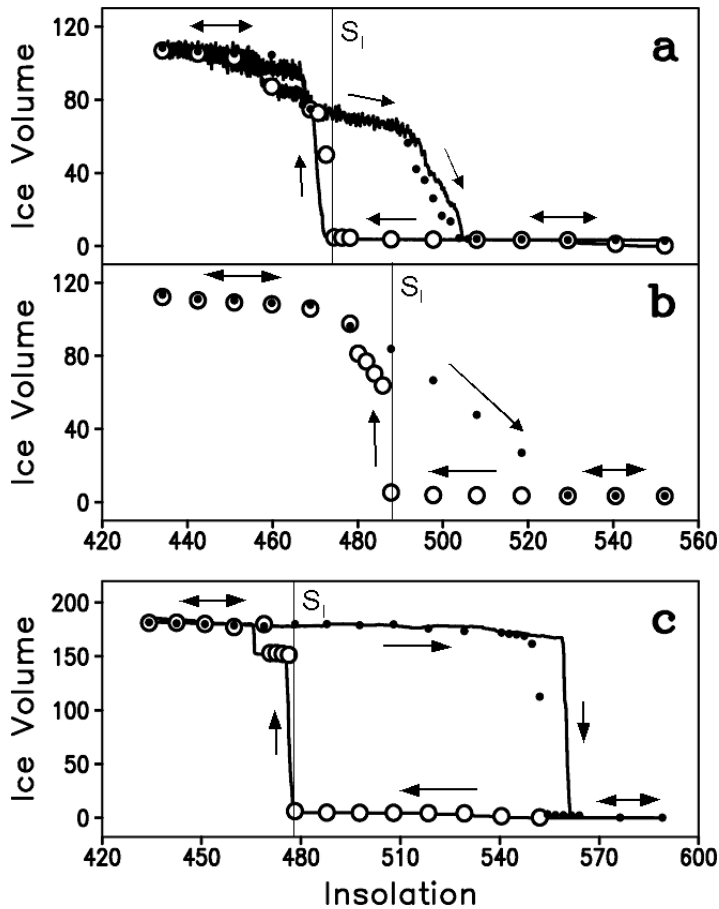
Figure 1. Inland-ice volume (10^6 km^3) in the Northern Hemisphere plotted versus maximum boreal summer insolation at 65°N (Milankovitch forcing, MF, in W m^{-2}). The open circles are from the equilibrium experiments with ice-free initial conditions and the full dots indicate the equilibrium experiments with the maximum ice cover, which corresponds to the state as indicated by the dot on the upper left side of the diagrams, as initial condition. The solid lines are from the two experiments with slowly varying Earth orbital eccentricity. The black arrows show the direction of the hysteresis loop. The thin vertical line indicates the position of the threshold S_I. See text for explanation. Simulations shown are with fast sliding parameterization using (a) 280 ppm and (b) 200 ppm atmospheric CO_2 content. Panel (c) shows simulations with the slow sliding parameterization and 280 ppm atmospheric CO_2 content. Please note the different scale of the x-axis in this panel.
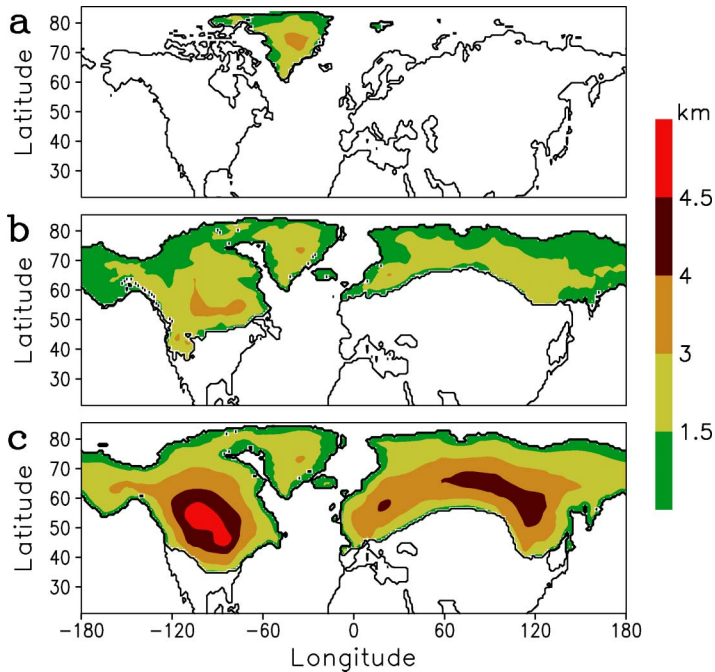
Figure 2. Ice-surface elevation on the Northern Hemisphere in km. All experiments in this figure are with MF = 488 W/m^2 and 280 ppm atmospheric CO_2 content. (a) Interglacial state with fast sliding. (b) Glacial state with fast sliding. (c) Glacial state with slow sliding.
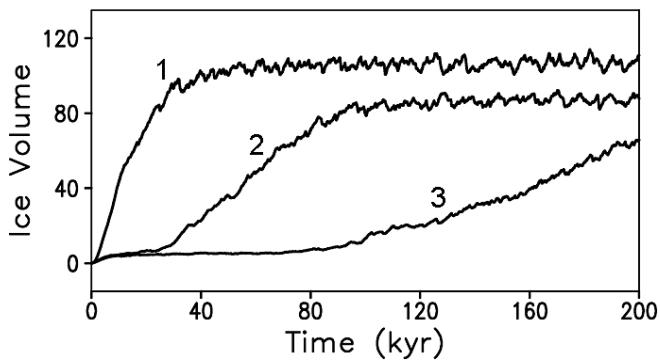
Figure 3. Transient response of a representative set of equilibrium experiments with fast sliding and pre-industrial atmospheric CO_2 concentration. Inland-ice volume in 10^6 km^3 and time in kyr (1000 years). Curves 1, 2 and 3 correspond to an MF of 434 W/m^2, 460 W/m^2 and 473 W/m^2, respectively.